

Pre-winter distribution and habitat characteristics of polar cod (*Boreogadus saida*) in southeastern Beaufort Sea

Delphine Benoit · Yvan Simard · Louis Fortier

Received: 18 March 2013 / Revised: 13 September 2013 / Accepted: 4 November 2013 / Published online: 4 December 2013
© Springer-Verlag Berlin Heidelberg 2013

Abstract Polar cod was shown to form dense under-ice winter aggregations at depth in the Amundsen Gulf (southeastern Beaufort Sea). In this paper, we verify the premises of the aggregation mechanism by determining the distribution and habitat characteristics of polar cod prior to the formation of winter aggregations. Multifrequency split-beam acoustic data collected in October–November 2003 revealed that polar cod split into two distinct layers. Age-0 polar cod formed an epipelagic layer between 0 and ~60 m depth without any clear large-scale biomass trend. In contrast, adult polar cod tended to distribute into an offshore mesopelagic layer between ~200 and 400 m that shoaled into a denser ($1\text{--}37\text{ g m}^{-2}$) benthopelagic layer on sloping bottoms (between 150 and 600-m isobaths) along the Mackenzie shelf and into the Amundsen Gulf basin. Concentrations peaked in the Amundsen Gulf where estimated total biomass reached ~250 kt. Both age-0 and adult polar cod distributed in the warmer waters ($>-1.4\text{ }^{\circ}\text{C}$). We hypothesise that polar cod concentration over slopes is

governed by the combined actions of (1) local currents concentrating both depth-keeping zooplankton and polar cod at the shelf-break and basin slopes and (2) trophic association with these predictable topographically trapped aggregations of zooplankton prey. During freeze-up, these slope concentrations of polar cod are thought to constitute the main source of the observed dense under-ice winter aggregations. The hypothesis of active short-distance displacements combined with prevailing mean currents is retained as the likely aggregation mechanism.

Keywords Polar cod · Shelf-break · Amundsen Gulf · Mesopelagic · Migration · Biomass estimate

Introduction

Polar cod (*Boreogadus saida*) is the most widespread and abundant fish of the Arctic Ocean (Lowry and Frost 1981; Craig et al. 1982; Bradstreet et al. 1986; Parker-Stetter et al. 2011). As the main forage species, it plays a key role in the marine ecosystem, by transferring up to 75 % of the zooplankton production to marine vertebrate predators (Welch et al. 1992). In seasonally ice-covered areas, adult polar cod primarily feed on late stages of pelagic zooplankton species (Lowry and Frost 1981; Craig et al. 1982; Lønne and Gulliksen 1989). Calanoid copepods such as *Calanus glacialis*, *Calanus hyperboreus*, and *Metridia longa* are the most frequent prey found in polar cod stomachs and constitute an important carbon intake for polar cod (Bradstreet et al. 1986; Benoit et al. 2010). Hyperiid amphipods are also part of the diet of polar cod but are occasional prey (Benoit et al. 2010). Juvenile polar cod preferentially feed on eggs and nauplii of calanoid copepods (Michaud et al. 1996).

D. Benoit (✉) · L. Fortier
Département de biologie, Université Laval, Québec,
QC G1V-0A6, Canada
e-mail: delphine.benoit.1@ulaval.ca

L. Fortier
e-mail: louis.fortier@bio.ulaval.ca

D. Benoit · Y. Simard
Institut des Sciences de la Mer, Université du Québec à
Rimouski, 310 allée des Ursulines, Rimouski, QC G5L 3A1,
Canada
e-mail: yvan_simard@uqar.ca

Y. Simard
Institut Maurice-Lamontagne, Pêches et Océans Canada,
850 route de la Mer, Mont-Joli, QC G5H 3Z4, Canada

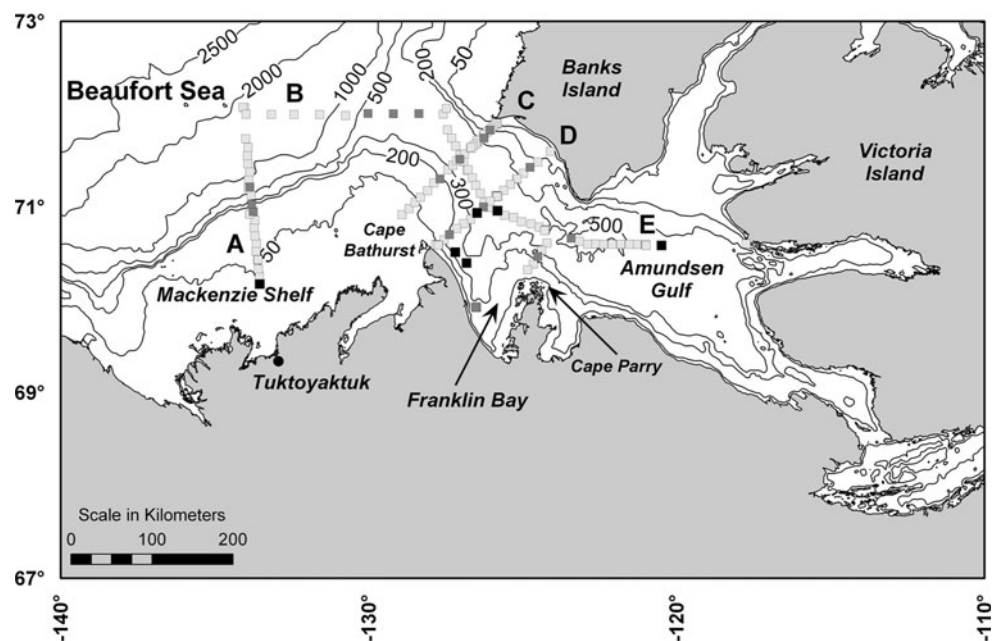
During the open-water season, polar cod were shown to form dense near-shore schools of adults and juveniles (e.g. Welch et al. 1993; Crawford and Jorgenson 1996; Parker-Stetter et al. 2011). Widespread layers of age-0 fish were found in the upper 75 m of the epipelagic zone, while aggregations of age-1 + distributed at depth at shelf-break (e.g. Cross 1982; Jarvela and Thorsteinson 1999; Geoffroy et al. 2011; Parker-Stetter et al. 2011). During winter, an exceptionally dense monospecific aggregation of adults (98 % of fish captured were polar cod) have been found under the consolidated sea-ice in deep waters (>200 m) in Franklin Bay in 2004 (Benoit et al. 2008). Similar winter aggregations were also detected along the northern slope of the Amundsen Gulf in 2007–2008 (Geoffroy et al. 2011). These aggregations persisted with varying densities from December to April. Polar cod always remained in the warmer waters of the Pacific Halocline and Atlantic Layer, where their copepod prey species were also most abundant. In May, when the midnight sun appeared, the dense, deep fish layer rose in the water column and started splitting into very dense schools, which gradually occupied the upper water column (Benoit et al. 2010), likely to follow the ontogenetic vertical migration of their copepod prey (Geoffroy et al. 2011). These overwintering polar cod aggregations are thought to result from bio-physical coupling involving conditioning during the early-winter spawning, passive advection, and depth-keeping behaviour to minimise predation mortality (Benoit et al. 2008, 2010). Near-spawning or spent polar cod concentrated on the slopes in early winter would be transported through the along-slope residual circulation of the Amundsen Gulf. As a result of their depth-keeping behaviour, they would

accumulate at sloping topographical features favouring retention, such as the deep Franklin Bay and other locations on the Amundsen Gulf slopes (Benoit et al. 2008).

The southeastern Beaufort Sea (69°–73°N; 110°–140°W) includes (1) the Mackenzie shelf and its offshore waters west of Cape Bathurst and (2) the Amundsen Gulf that widely opens on the Canada Basin on the West and connects with the Canadian Archipelago through narrow straits south of Victoria Island and East of Banks Island (Fig. 1). The Mackenzie shelf extends over ~150 km before the shelf-break, where depths drop to >1,000 m in less than 50 km. The adjacent Amundsen Gulf is a 400–600 m deep opening into the shelf where the bottom quickly steepens all around the coastline, entailing a much narrower shallow-water area.

Surface circulation is forced by the anticyclonic atmospheric circulation that drives the Beaufort Gyre, creating a westward flow off the shelf slope (Lukovich and Barber 2006). Surface waters generally enter the Amundsen Gulf along Cape Bathurst and flow out south of Banks Island (Barber et al. 2010). This circulation pattern occasionally reverses, as observed in 2003 (Lanos 2009). At depth (>150 m), circulation is under the influence of the Beaufort undercurrent flowing eastward along the shelf slope, then running southward at the head of the Amundsen Gulf before flowing out along the northern slope (Aagaard 1984; Kulikov et al. 1998). On the Mackenzie shelf (Fig. 1), circulation is generally eastward (Carmack and MacDonald 2002). The water column in the eastern Beaufort Sea splits up into three water masses: the Polar Mixed Layer (0–50 m), the Pacific Halocline (50–200 m), and the deep Atlantic Waters (>200 m). Freeze-up starts in October with

Fig. 1 Bathymetric map of southeastern Beaufort Sea. Isobaths are in metres. *Light grey squares* indicate locations of CTD casts and echointegration analysis. *Dark grey squares* indicate stations where TS analysis was performed. *Black squares* indicate net tows where polar cod were captured. All *dark grey squares* and *black squares* overlay *light grey squares*. Five main transects are designated as capital letters (A–E)



the formation of land-fast ice that spreads along coasts. By December, the ice cover is consolidated (Barber and Hanesiak 2004; Galley et al. 2008).

In the present paper, we test the assumption that polar cod were mainly distributed at the slopes of the south-eastern Beaufort Sea prior to sea-ice consolidation in fall 2003 and subsequent observation of the Franklin Bay overwintering aggregation in 2004. We examine the horizontal and vertical distributions of age-0 and adult polar cod in the southeastern Beaufort Sea during October–November 2003. We also provide an estimation of the adult polar cod stock in the Amundsen Gulf, and we investigate the relations between polar cod biomass and depth, isobaths, and thermal structure of the water masses.

Materials and methods

Hydrography

As part of the Canadian Arctic Shelf Exchange Study (CASES), the research icebreaker CCGS *Amundsen* surveyed the southeastern Beaufort Sea from 18 October to 20 November 2003 along five main transects (Fig. 1). The study area covered bottom depths ranging from 30 to 1,900 m. A conductivity-temperature-depth (CTD) probe rosette system (Seabird SBE-911[®]) was deployed at 108 stations (Fig. 1) to a maximum depth of 1,187 m. Some stations were sampled several times leading to 147 CTD casts. For each of these profiles, temperature and salinity were averaged over 3-m bins to correspond to the vertical resolution of the fish biomass echo-integration bins (see below) and the resulting profiles were used to identify the different water masses. Along-transect cross-sections of temperature and salinity were contoured with Ocean Data View © 4.3.1, using the Data-Interpolating Variational Analysis method (DIVA software, Université de Liège, Belgium) with specified correlation length scales. This same contouring method was applied to the estimated polar cod biomass.

Ichthyoplankton sampling and analysis

When ice conditions allowed, a sampler consisting of 2 square nets (1 m² aperture, 0.5 and 1.6 mm mesh) mounted side by side on a metal frame was towed obliquely in the surface layer (0–100 m) to collect ichthyoplankton. This sampler was deployed eleven times during the survey and collected polar cod on 6 tows. A second similar sampler dedicated to zooplankton sampling was mounted with smaller mesh (0.2 and 0.5 mm). This sampler was towed vertically to a maximum depth of 390 m and collected ichthyoplankton on two occasions. A total of 23 age-0

polar cod were caught among the 26 fish collected at 6 stations (Fig. 1).

Fish standard length (SL) was measured on mm-gridded paper. The fork lengths (FL) of age-0 polar cod were obtained from a regression ($FL = 1.0578SL - 0.0714$; $r^2 = 0.996$) we established from 43 polar cods collected in the Laptev Sea in September 2005 (Bouchard and Fortier 2008). FLs of age-0 polar cod were used to calculate their weight using the weight–FL relationship from Rand and Logerwell (2010) and calculate their theoretical target strength (TS, see below) from the TS–FL relationship from Parker-Stetter et al. (2011).

Sampling and analysis of acoustic data

The acoustic data acquisition setup is described in Benoit et al. (2008). Briefly, the CCGS *Amundsen* is equipped with a Simrad EK60 multifrequency (38, 120 and 200 kHz, all 7° beam width) split-beam echosounder calibrated with the standard sphere method (Foote et al. 1987) that was continuously recording the backscatter from the water column during the survey. Ping interval varied from 3 to 4 s, and pulse duration was 1,024 μs.

The on-course acoustic data are often contaminated by noise and interferences due to vessel noise, vessel speed, ice-breaking and manoeuvres, sea-state, transducer aerations, etc. The data used in this paper are relatively independent of such on-course noise because they only correspond to periods when the ship was slowly moving or stopped at stations during CTD cast. At each station, 1 h of acoustic data was selected around each CTD-rosette cast, which allows a close pairing with the environmental variables. This subsampling provided 145 h of acoustic data corresponding to the surveyed CTD station grid.

The EK60 raw files were converted to the international standard hydroacoustic (HAC) format (Simard et al. 1997). The HAC files were edited to exclude any corrupted data following Benoit et al. (2008), and a time-varied threshold was inserted to exclude background noise using CH2 software (Simard et al. 2000). Echointegration was performed at 38 and 120 kHz for each 1-h subsample (Simmonds and MacLennan 2005). Echointegration cells were 20-pings wide (i.e. 60–80 s) and 3-m high. Time-varied gain was based on the actual sound speed and absorption coefficient (Francois and Garrison 1982) for each frequency, calculated from temperature, salinity and sound speed profiles averaged over the water column for all stations. The echointegration was done in volume scattering strength units (S_V in dB re 1 m⁻¹) using a minimum threshold of -90 dB.

Sea-ice conditions at that period of the year make deployment of trawls difficult. Hence, no fish samples from the mesopelagic zone were available to ground-truth the

acoustic data. However, in the Beaufort Sea pelagic zone, polar cod dominates the fish community (Craig et al. 1982; Rand and Logerwell, 2010; Parker-Stetter et al. 2011) and zooplankton is mainly composed of small fluid-like sound scattering organisms (Benoit et al. 2008). To discriminate polar cod from zooplankton, we used the dB-differencing method in S_V computed at 38 and 120 kHz ($\Delta S_{V120-38}$) for each echointegration cell (e.g. Kang et al. 2002). This method takes advantage of the frequency-dependent back-scattering signature characterising different types of organisms (e.g. Holliday and Pieper 1995; Horne 2000; Lavery et al. 2007) and has been proven to effectively distinguish swimbladdered fish from fluid-like zooplankton (e.g. Madureira et al. 1993; Simard and Lavoie 1999). $\Delta S_{V120-38}$ of juveniles and adult swimbladdered fish generally ranges from -10 dB to 5 dB (Kang et al. 2002; Logerwell and Wilson 2004; Murase et al. 2009), while the $\Delta S_{V120-38}$ of copepods and large amphipods, dominating the local zooplankton, is generally >5 dB (Madureira et al. 1993; Kang et al. 2002; Murase et al. 2009; Simard and Sourisseau 2009). To avoid noisy estimates and ensure a good signal-to-noise ratio, the $\Delta S_{V120-38}$ was computed using a threshold of -90 dB at both frequencies. A $\Delta S_{V120-38}$ ranging from -10 to 5 dB was considered as polar cod. More than 93 % of $\Delta S_{V120-38}$ values ranged from -10 to 5 dB. Modal values of $\Delta S_{V120-38}$ were -3.5 dB close to the surface (0 – 60 m), and -2.5 dB in the deeper water column (150 – 600 m).

Polar cod biomass (g m^{-3}) was calculated with a conversion factor, TS_W ($TS_W = -29.59 \text{ dB kg}^{-1}$; Benoit et al. 2008), applied to 38-kHz S_V on echointegration cells having a $\Delta S_{V120-38}$ ranging from -10 to 5 dB. Biomasses were converted to number of fish using a 28.4 g mean weight per adult polar cod (Benoit et al. 2008), and 1.1 g mean weight per age-0 polar cod. This latter value was obtained by converting the SL distribution of captured age-0 polar cod during this survey using the weight–FL relationship established by Rand and Logerwell (2010) and our FL–SL linear regression.

Target strength analysis

An in situ target strength (TS) analysis was performed to (1) compare the TS signature of individual fish with previously validated polar cod echoes and to (2) examine the depth-dependant variations of TS values. A subsample of 17 stations, totalling 17 h, was selected from the 145 h of acoustic data retained for echointegration. These 17 stations were selected in order to maximise the spatial coverage and include different bathymetric conditions (Fig. 1). All subsampled stations corresponded to night time to ensure a maximum dispersion of fish (Benoit et al. 2010). The analysis was performed with Echoview[®] 5.2 (Myriax Software, Hobart, Tasmania) on the 38 kHz data,

Table 1 Parameters used in Echoview[®] for the target strength (TS) analysis at 38 kHz (Single-target detection and fish tracking)

Parameter	Value
<i>Single-target detection algorithm</i>	
Threshold (dB)	-65
Min. normalised pulse length	0.7
Max. normalised pulse length	1.3
Max. beam compensation (dB)	6
Max SD of minor-axis angle (degrees)	0.6
Max SD of major-axis angle (degrees)	0.6
<i>Fish tracking algorithm</i>	
Min. number of single targets in a track	3
Min. number of pings in a track (pings)	3
Max. gap between single targets (pings)	2

which is better suited for fish detection. Echoview[®] single-target detection algorithm for split-beam echosounder (method 2: threshold applied on targets after compensation for their position in the beam) was used to extract single targets and calculate their TS. A TS threshold of -65 dB was used to exclude zooplankton echoes. Single-target detection criteria were tuned to maximise the number of detected targets and minimise multiple target detections (Table 1). The low ship speed on stations allowed the recording of long traces of individual fish, while they cross the beam for several pings. The Echoview[®] fish tracking algorithm was applied on extracted single targets to obtain the mean TS value of individual fish traces. This method has the advantage of reducing the stochastic error of the individual measurements (Simmonds and MacLennan 2005).

Results

Thermohaline water mass characteristics

The vertical distribution of water masses over the study area (Fig. 2) included the Polar Mixed Layer (PML, $S < 32.5$) in the first 50 – 100 m of the upper water column where temperatures ranged from -1.6 to 0.9 °C depending on locations. Below, the Cold Halocline ($T < -1.4$ °C; $32.5 < S < 33.5$) extended down to 200 m and spread over the Mackenzie shelf, with tilted contours typical of upwelling (Fig. 2, transects A, C and D). The lower Pacific Halocline ($-1.4 < T < 0.3$ °C; $33.5 < S < 34.7$) went down to ca. 300 m and impinged on slopes in continuity with the tilted upwelling layer on the Mackenzie shelf edges. Below 300 m, the relatively warm (> -0.3 °C) and saltier (> 34.5) Atlantic layer occupied the remainder of the water column in the central Amundsen Gulf and off the Mackenzie shelf.

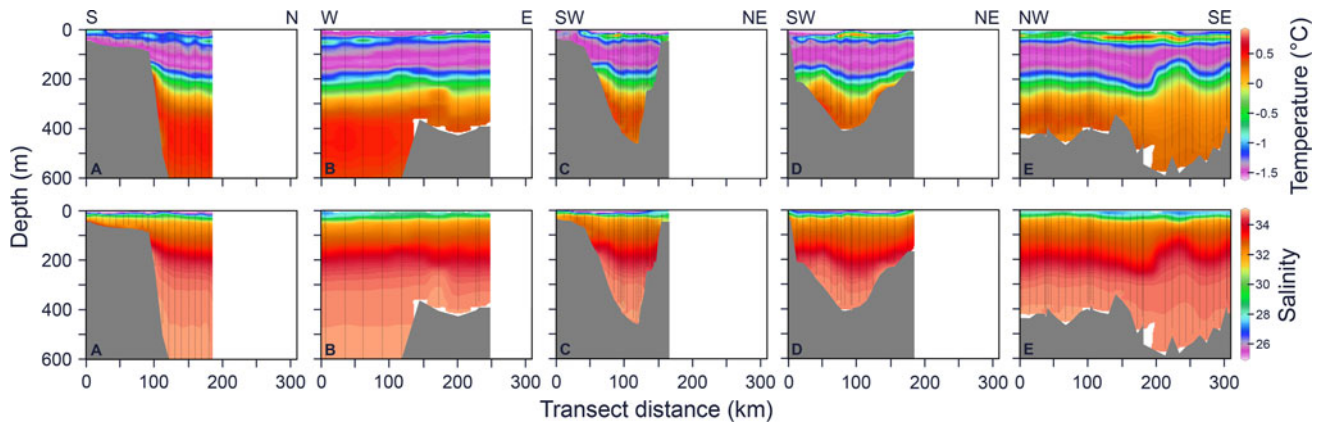


Fig. 2 Along-transect (distance, km) distribution of temperature ($^{\circ}\text{C}$, upper panels) and salinity (psu, lower panels) versus depth (m) for main transects (from left to right, A–E). Black vertical lines indicate

CTD casts. The grey area represents sea bottom. Letters on top of temperature panels indicate cardinal directions of transects

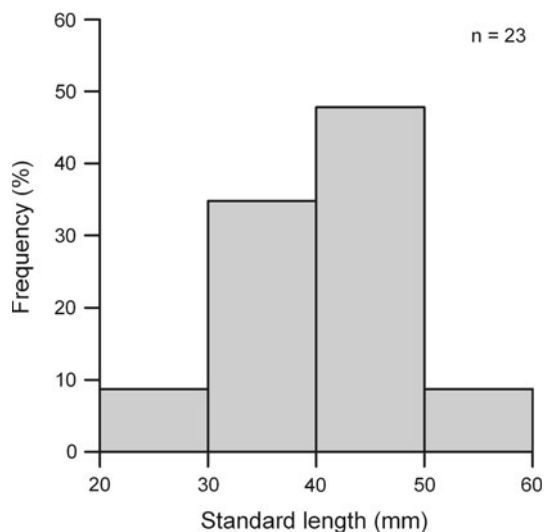


Fig. 3 Standard length (mm) frequency distribution of net-captured juvenile polar cod

Age-0 polar cod in the epipelagic layer

Out of the 26 individual fish sampled, age-0 polar cod constituted 88.5 % of the ichthyoplankton collected in the epipelagic layer. Their standard lengths ranged from 25.5 to 51.5 mm (mean \pm SD: 41.7 ± 7.1 mm) (Fig. 3). Corresponding fork lengths ranged from 26.9 to 54.4 mm (mean \pm SD: 44.0 ± 7.5 mm).

Polar cod biomass

Polar cod were vertically distributed in two distinct layers defined by biomasses $>0.02 \text{ g m}^{-3}$ (Fig. 4). An epipelagic layer distributed between 0 and 60 m (Fig. 4) with areal biomasses averaging 0.5 g m^{-2} (Table 2). In this layer, polar cod areal biomasses showed no clear spatial trend

among analysed stations except for lowest densities far offshore (Fig. 5a), and displayed little variations with bathymetry (Fig. 6a). The sizes of the densest patches extended from ~ 50 to 100 km (Fig. 4).

A mesopelagic layer primarily occupied depths between about 200 and 400 m (Fig. 4), with areal biomasses ranging from 0.02 to 36.98 g m^{-2} and averaging 3.12 g m^{-2} (Table 2). Unlike the epipelagic layer, biomasses presented notable bathymetric and spatial variations (Figs. 5b, 6b). Highest areal biomasses (2.8 – 5.3 g m^{-2}) were concentrated at bottom depths ranging from 150 to 600 m (Fig. 6b). Corresponding standard deviations increased accordingly and were proportionally higher (CV = 119 %) in the 350–450 m layer, reflecting a higher variability in this bathymetry class. Over bottom depths <150 m (continental shelf shallows) or >600 m, polar cod areal biomasses were noticeably lower ($<1.5 \text{ g m}^{-2}$) (Fig. 6b). Biomasses peaked (up to 37 g m^{-2}) in the Amundsen Gulf, particularly in the central depression and on the slopes (Fig. 5b). Outside the Gulf, biomass increased at the crossing of the slope (up to 3.4 g m^{-2}) and the 500-m isobaths at the head of the Amundsen Gulf (up to 3.2 g m^{-2}) (Figs. 4, 5b). Off slope, biomasses were rather low ($<2.7 \text{ g m}^{-2}$). The mesopelagic layer was essentially associated with the bottom on the slopes (Fig. 4, transects A, B, C and D) but a part of it was only pelagic in deeper areas (Fig. 4, transects B, C, D, E).

When the zones where the biomass is negligible ($<0.02 \text{ g m}^{-3}$) are ignored (84 %), the mean biomass in waters occupied by polar cod becomes 0.04 g m^{-3} in the epipelagic layer and 0.05 g m^{-3} in the mesopelagic layer (Table 2). The Pearson correlation coefficient showed no significant relationship (<0.1 ; $p > 0.05$) between the areal epipelagic and mesopelagic biomasses, which indicates the de-coupling between the regional distributions of the two fish sizes.

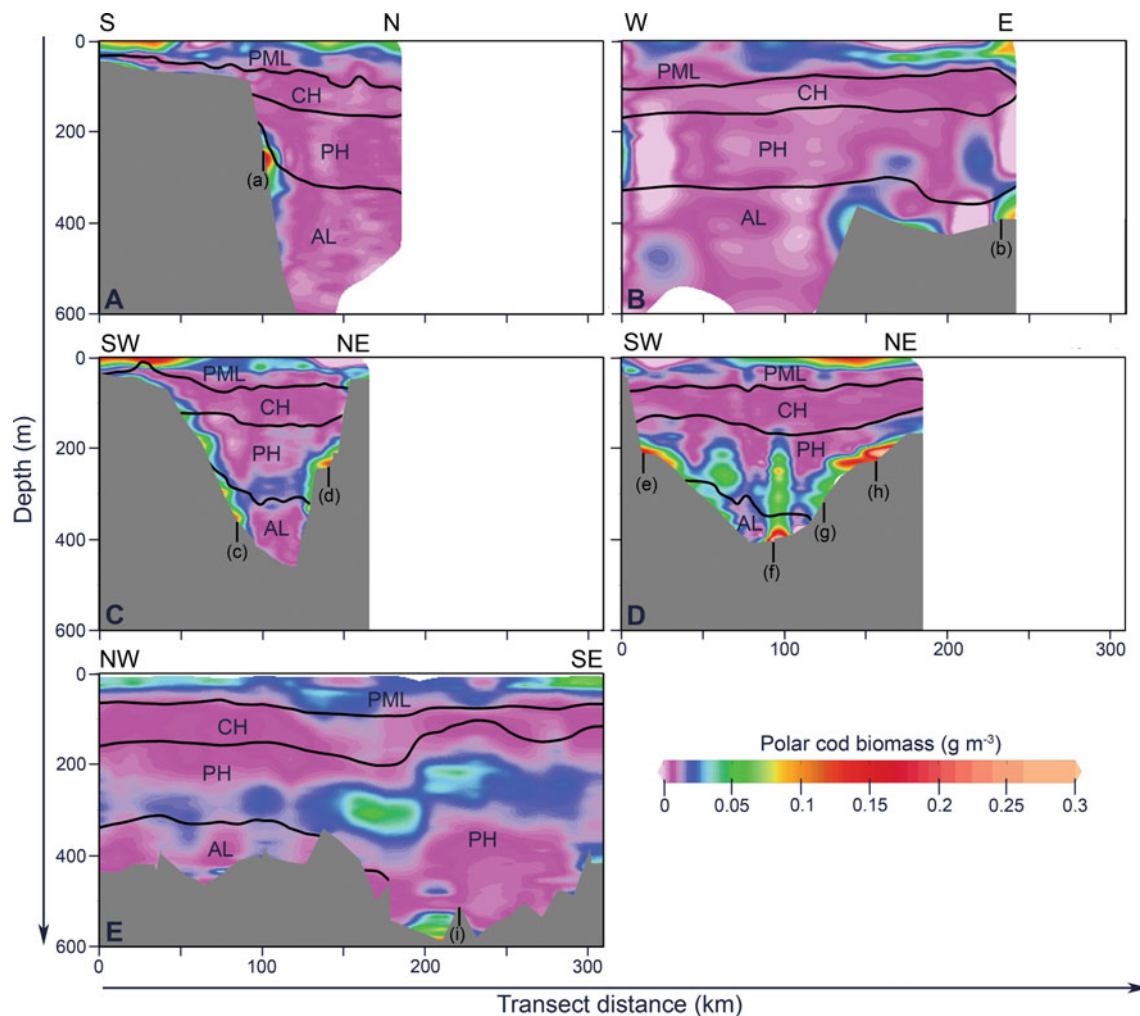


Fig. 4 Along-transect (distance, km) distribution of polar cod biomass (g m^{-3}) versus depth (m) for transects A–E corresponding to Fig. 1. Solid black lines delineate water masses (PML Polar Mixed Layer, CH Cold Halocline, PH Pacific Halocline, AL Atlantic Layer).

The epipelagic age-0 polar cod was located in the Polar Mixed Layer that corresponds to warm (> -1.4 °C) and low-salinity (< 32.5) waters, except at the very surface (Fig. 7). 77 % of echointegration cells having a significant polar cod biomass (> 0.02 g m^{-3}) were in water temperatures ranging from -1.4 to -0.1 °C, around a modal temperature of -1.05 °C (Fig. 8a). The mesopelagic polar cod were distributed mostly in the Pacific Halocline and Atlantic layer, where water temperatures and salinities increase with depth (respectively, from -1.4 °C to ~ 0.5 °C and 33.5 to 34.9) (Fig. 7). 81 % of echointegration cells having a significant polar cod biomass (> 0.02 g m^{-3}) were in water temperatures ranging from -0.4 to 0.4 °C, around a modal temperature of 0.15 °C (Fig. 8b). In the Cold Halocline, where temperatures come within reach of the freezing point, polar cod were very scarce (Figs. 4, 7). Polar cod occupied this layer at a few stations, when deep upwelling conditions were encountered (Figs. 2, 4, transects A and C).

Note that colour scale is not linear. The grey area represents sea bottom. Capital letters on top of panels indicate cardinal directions of transects. Lowercase letters and vertical dash indicate location of selected casts for Fig. 7

Target strengths

The TS distribution through the water column at night was characterised by 2 modes separated at a value of ~ -50 dB (Fig. 9a). A low-TS mode gradually died out with increasing depth and was replaced by a high-TS mode (Fig. 9a). Between 0 and 200 m, the low-TS mode shifted from -57.25 to -54.75 dB and became indistinguishable below 250 m. The high-TS mode gradually appeared between 100 and 200 m before completely emerging at deeper depths. Its modal value increased with depth from -49.25 to -41.25 dB. Down to 150 m, where high-TS values were almost absent, mean TS of tracks averaged -54.68 dB. As expected from the increasingly larger volume sampled by the acoustic beam with depth, the number of single-target detections in the beam decreased with depth. Since these in situ TS tracks were collected during the night, when nocturnal dispersion occurs, the average

Table 2 Polar cod densities calculated from mean biomass estimates at each station

	<i>n</i>	Minimum	Maximum	Mean	SE (%)	Median	1st quartile	3rd quartile
<i>Whole water column</i>								
Density (g m ⁻²)	145	0.15	37.12	3.25	9.1	3.25	0.77	4.23
Density (g m ⁻³)	13,539	0.001	0.985	0.015	1.5	0.008	0.006	0.015
Density ^a (g m ⁻³)	2,201	0.020	0.985	0.047	2.4	0.032	0.024	0.048
<i>Epipelagic layer</i>								
Density (g m ⁻²)	145	0.04	1.75	0.49	5.1	0.44	0.26	0.65
Fish ^b (m ⁻²)	145	0.04	1.64	0.46	5.1	0.41	0.25	0.61
Density (g m ⁻³)	1,924	0.001	0.182	0.017	9.1	0.012	0.008	0.019
Fish ^b (m ⁻³)	1,924	0.001	0.171	0.016	2.2	0.011	0.008	0.018
Density ^a (g m ⁻³)	462	0.020	0.182	0.038	2.8	0.029	0.024	0.042
<i>Mesopelagic layer</i>								
Density (g m ⁻²)	128	0.02	36.98	3.12	10.3	2.86	1.38	3.79
Fish ^c (m ⁻²)	128	<0.01	1.3	0.11	10.3	0.10	0.05	0.13
Density (g m ⁻³)	11,615	0.001	0.985	0.014	1.7	0.008	0.005	0.014
Fish ^c (m ⁻³)	11,615	<0.001	0.035	<0.001	1.7	<0.001	<0.001	<0.001
Density ^a (g m ⁻³)	1,739	0.020	0.985	0.049	2.8	0.033	0.024	0.049

^a For values >0.02 g m⁻³

^b Based on 28.4 g per fish

^c Based on 1.1 g per fish

daytime vertical distribution is likely different with a sharper depth separation between the two modes, as the general biomass distribution of the epipelagic and the mesopelagic fish layers showed (Fig. 4).

The TS were grouped in three significantly different (Kruskal–Wallis, $p < 0.01$) depth layers, distinguishing the low- and high-TS modes and the mixed zone, (Fig. 9b). In the epipelagic layer (0–60 m), the low-TS mode was symmetrically centred on a modal value of –57.25 dB, with fish track mean TS of –56.68 dB (SD = 2.06 dB). In the upper mesopelagic layer (60–250 m), a strong low-TS mode was also observed but it was shifted upward by ~+2 dB (modal value = –55.25 dB), and higher modes (centred at –48.75 dB and possibly 44.25 dB) lined up in the distribution in contrast with the epipelagic layer. Overall, the TS distribution ranged from –63.36 to –35.28 dB in the upper mesopelagic layer (mean = –49.28 dB). In the deeper mesopelagic layer (>250 m), only high-TS values (from –55.25 to –35.37 dB) were found, with fish track mean TS of –49.28 dB and modal value of –44.25 dB, and they merged into a single, slightly skewed mode.

Discussion

Depth segregation of polar cod population

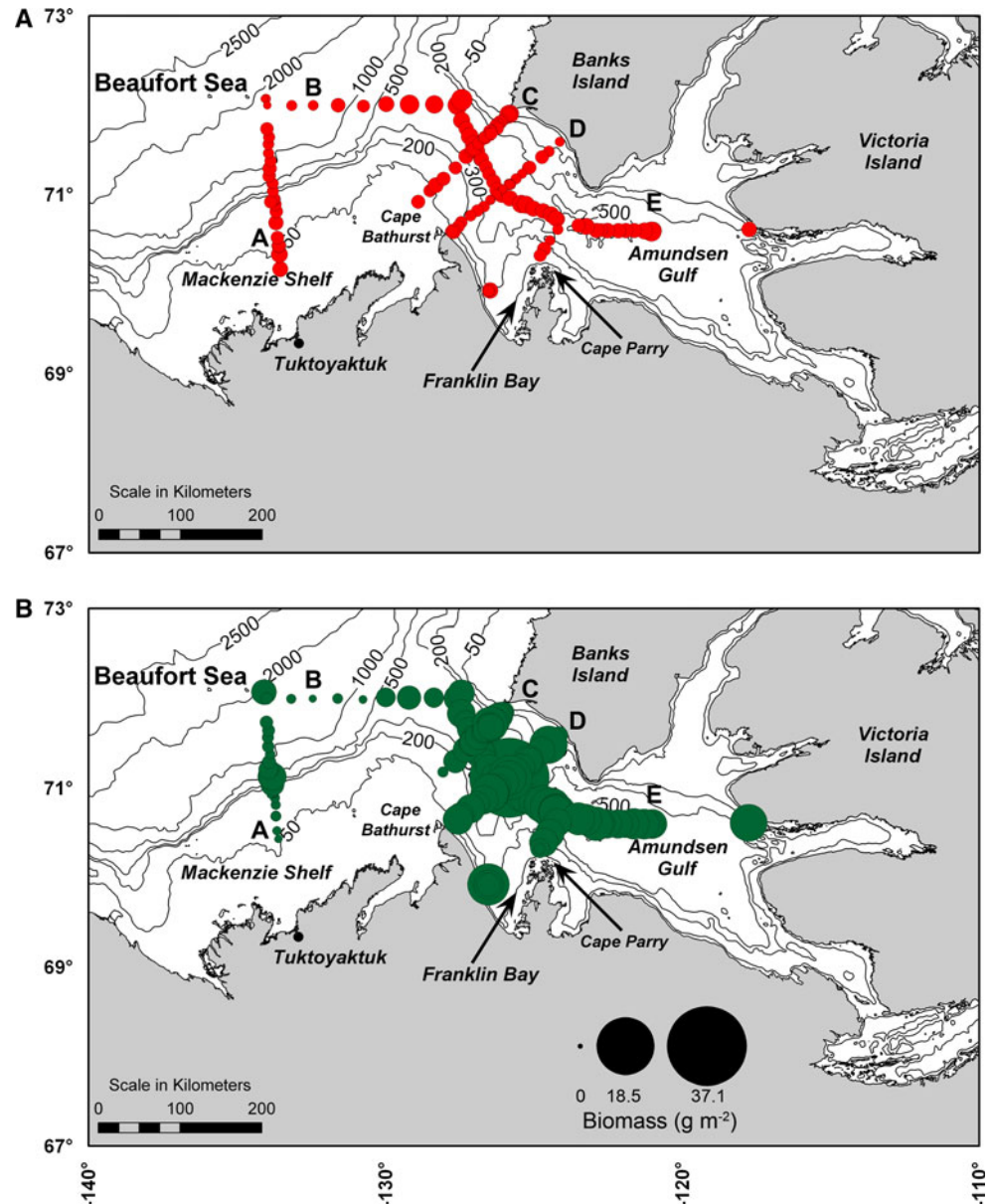
Multi-frequency echointegration revealed two distinct and largely widespread fish layers. Complementary information

on their respective fish sizes was provided by the in situ TS analysis. The mean in situ TS value (–56.7 dB) in the epipelagic layer closely matches the TS estimated (–55.6 dB) for the net sampled age-0 polar cod (fork length = 4.4 cm) using the TS–length relationship established by Parker-Stetter et al. (2011) for these small fish. The mean TS within the 0–150 m depth layer differ by only 0.5 dB from that observed 5–6 months later in Franklin Bay for the top (0–140 m) of the net-validated polar cod aggregation (Benoit et al. 2008; Geoffroy et al. 2011). These TS values, respectively, correspond to 6.7 and 7.2 cm fish from Crawford and Jorgenson (1996)'s TS–length relationship for adult polar cods.

Below 150 m, the in situ TS gradually increased with depth with modal values ranging from –49.25 to –41.25 dB below 200 m. These TS correspond to polar cod lengths ranging from 11.9 to 27.7 cm (Crawford and Jorgenson 1996), which is also very similar to the 11.6–25.9 cm polar cod caught between 130 and 220 m depths within Franklin Bay winter aggregation a few months later (Benoit et al. 2008). The possibility of a depth-dependent bias from the in situ TS split-beam method, where the noise amplified by the TVG (Time-Variied Gain) would progressively mask weaker echoes with increasing depth (Ona 1999) can be ruled out. Such an effect would gradually truncate the low values tail of the in situ TS distribution with depth, which is not observed.

The widespread distribution and the correspondence of our in situ TS with validated polar cod TS support polar

Fig. 5 Spatial distribution of polar cod biomass (g m^{-2}) in southeastern Beaufort Sea between 18 October and 20 November 2003 for **a** the epipelagic layer (depth < 60 m) and **b** the mesopelagic (depth > 60 m) layer. *Dots* area is proportional to biomass



cod as the dominant species composing the fish layers we observed. Besides, the depth segregation of polar cod sizes we observed is in agreement with other observations of two size-segregated distinct polar cod layers (Sekerak 1982; Falk-Petersen et al. 1986; Ponomarenko 2000; Parker-Stetter et al. 2011). We are therefore confident that polar cod was the dominant source of the observed fish layers.

Moreover, the depth segregation of the polar cod population reflects size/age differences in habitat use. Age-0 epipelagic polar cod were associated with warm and low-salinity water, while adults in the mesopelagic layer were also associated with warm but saltier water at depth (Fig. 7). This distribution pattern thus re-emphasises the importance of temperature for this arctic species (Benoit

et al. 2008; Bouchard and Fortier 2008), and, most importantly, suggests that the small juveniles delay as much as possible (i.e. until the surface layer becomes too cold) their rendezvous at depth with their progenitors. The gradual increase in TS values with depth in the first 200 m of the water column especially evidences this ontogenetic migration and suggests the need for age-0 polar cod to reach a minimum size before their descent to greater depths. No epipelagic backscatter was observed in Franklin Bay during the months following this fall survey (Benoit et al. 2008; 2010), indicating that surviving age-0 individuals may have completed their descent to greater depths by December. Further in situ investigations on this ontogenetic vertical migration of polar cod should therefore focus on this pre-winter period.

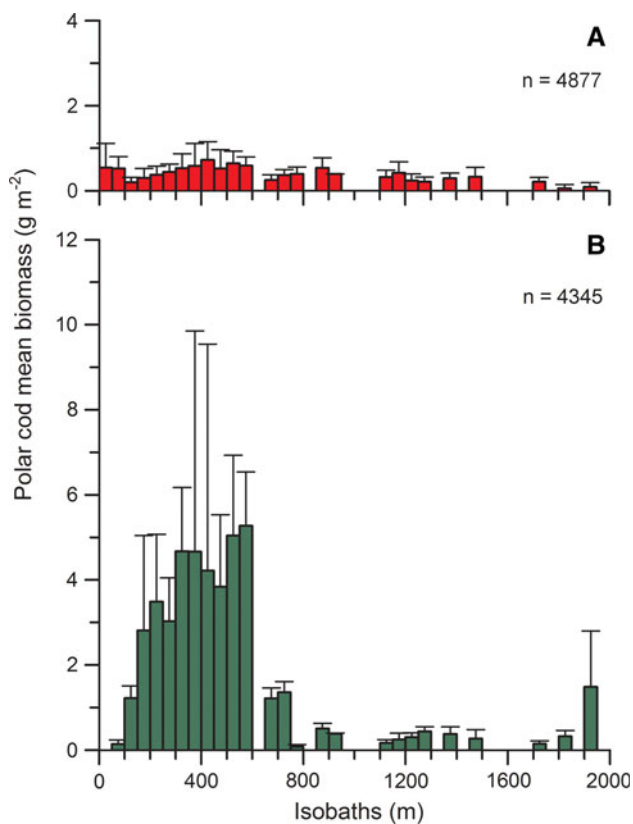


Fig. 6 Mean polar cod biomass (g m^{-2}) per isobath class (m) for **a** the epipelagic layer and **b** the mesopelagic layer. Vertical bars indicate standard deviation

Pre-spawning polar cod concentrations, total biomass and behaviour

During our sampling period (18 October to 20 November 2003), the adult polar cod distributed near the bottom in slope areas were very likely at pre-spawning stage. Gonad development starts in August (Hop et al. 1995) and polar cod spawn mainly in January–February under the sea-ice cover (Ponomarenko 1968; Rass 1968). In 2004 in the Beaufort Sea, the hatching period of offshore larvae was estimated to be between April and June (Lafrance 2009). Given an egg incubation time varying from 45 to 90 days (Rass 1968), spawning would have occurred from January to mid-April 2004.

During the 2003 freeze-up period in the southeastern Beaufort Sea, pre-spawning polar cod did not form dense aggregations as those reported for winter in Franklin Bay ($10\text{--}2,700 \text{ g m}^{-3}$, Benoit et al. 2008), and the northern slope of the Amundsen Gulf ($2\text{--}27 \text{ g m}^{-3}$, Geoffroy et al. 2011). Our maximum pre-winter estimate was only 1 g m^{-3} , and biomasses averaged 0.05 g m^{-3} ($\text{SE} = 2.8 \%$) within concentrations of polar cod (biomasses $>0.02 \text{ g m}^{-3}$). This large difference in polar cod density within a few months highlights the large change in prey density that predators

would face after freeze-up. Moreover, our observation of absence of dense aggregations over a large surveyed area prior to the consolidation of the ice cover concurs with Geoffroy et al. (2011)'s proposed link between the aggregation process and ice coverage. Winter aggregations observed in late January to April 2004 under the sea-ice cover at a 225-m deep station in Franklin Bay were composed of spent polar cod (Benoit et al. 2008). The similar aggregations of polar cod found on the northern slope of the Amundsen Gulf, south of Banks Island in winter 2008 appeared only after the ice cover was consolidated (Geoffroy et al. 2011).

The Amundsen Gulf hosted higher polar cod areal biomasses than the Mackenzie shelf slope. The area corresponding to the 150–600 m isobath in the Amundsen Gulf is $79,200 \text{ km}^2$. With a mean mesopelagic adult polar cod areal biomass of 3.12 g m^{-2} , the polar cod stock in the Amundsen Gulf would have approached 247 104 tons ($\text{SE} = 10.3 \%$) during the freeze-up period. For the ~ 16 times much larger Barents Sea (1.3 million km^2), polar cod stock has varied from 0.2 to 3 million tons between 1986 and 2006 (Gjøsæter et al. 2009), which corresponds to $\sim 1\text{--}12$ times our estimate. Despite its smaller area, the Amundsen Gulf stock estimate reaches that of the Barents Sea in low-abundance years. The Amundsen Gulf therefore appears to contribute to the Canadian Arctic hosting relatively high biomasses of the main forage species of the Arctic food web. Other parts of the Canadian Arctic Archipelago, notably Lancaster Sound, also host high polar cod biomass (Welch et al. 1992). The total polar cod stock in the Canadian Arctic could therefore be comparable with that of the Barents Sea.

We estimated polar cod biomass using the conversion factor TS_w calculated by Benoit et al. (2008) from adult polar cod (total lengths ranging from 11.6 to 25.9 cm) sampled in the same area (Franklin Bay) a few months later (April, May 2004). We assumed that the polar cod population in October–November had the same size distribution as in winter. In the alternative case that smaller individuals were present in the surveyed area, abundance in ind. m^{-3} or ind. m^{-2} would be under-estimated and, conversely, over-estimated in the case of larger mean fish. However, the biomass in g m^{-2} or g m^{-3} would be less affected because the change in the number of fish per kg is to some extent compensated by change in fish TS.

Possible mechanisms for the formation of aggregations

Benoit et al. (2008) suggested that passive transport of sluggish overwintering spent polar cod along slopes must have led to the accumulation observed in Franklin Bay. The head of the Amundsen Gulf was proposed as the origin based on the eastward deep circulation. Taking into

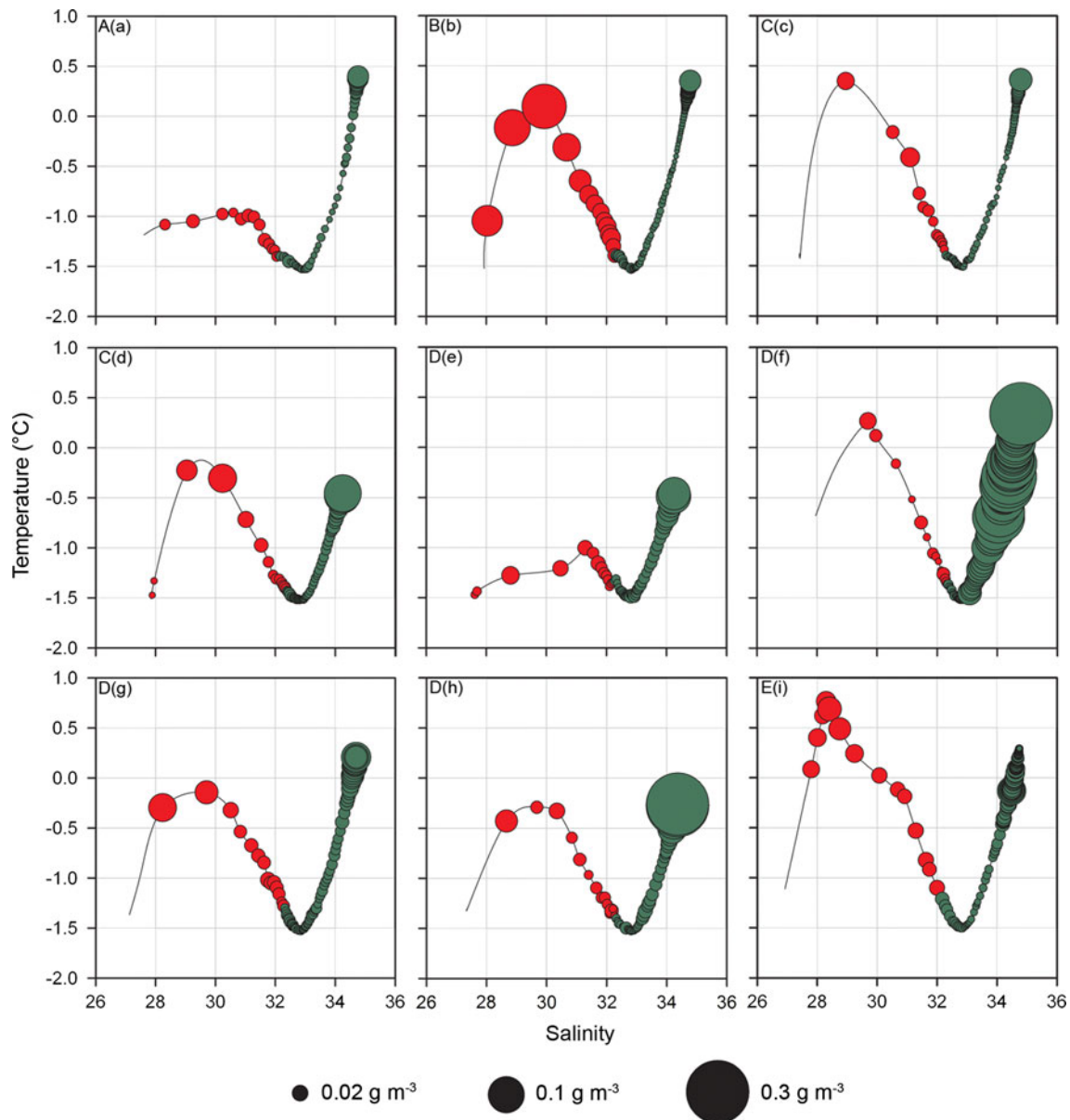


Fig. 7 Symbol plot of polar cod biomass (g m^{-3}) in the temperature–salinity diagram at 9 selected stations (**a–i**, corresponding locations on Fig. 4, capital letters are for transect names) in the study area. Dots size is proportional to biomass averaged over 1 h

using a 3-m vertical resolution. Estimated biomasses for the epipelagic layer (depth < 60 m) are represented as red circles, and green circles for the mesopelagic layer (depth > 60 m)

account a typical eastward residual circulation of 5 cm s^{-1} along the shelf-break (Pickart 2004), and that the formation of the aggregation lasted 2 months (Benoit et al. 2008), fish would have been carried from a radius of 260 km from Franklin Bay, which corresponds to the head of the Amundsen Gulf. Moreover, the thermohaline habitat of the observed benthopelagic adult polar cod was the same as that of overwintering individuals found several months later in Franklin Bay (Benoit et al. 2008). As hypothesised by Benoit et al. (2008), these adult polar cods preferentially

occupied the slope areas, remained close to the bottom, and were associated with the warmer waters of the Pacific Halocline and Atlantic Layer. All this supports the hypothesis that the polar cod we observed at depth probably constituted the source of the individuals that later formed a dense winter aggregation in Franklin Bay.

An alternative hypothesis to this principally passive transport is an active migration. Several fish species perform long-distance migrations towards specific spawning or feeding grounds [Atlantic cod (Hovgård and Christensen

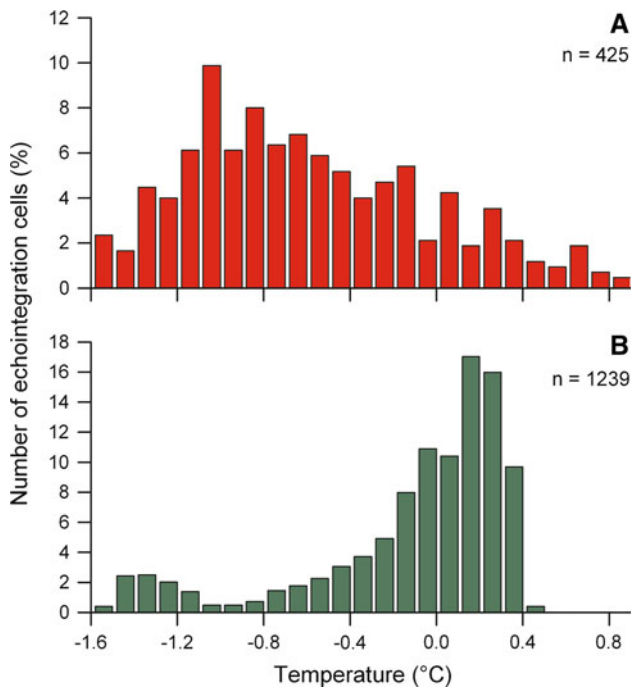


Fig. 8 Frequency distribution of significant polar biomass values ($>0.02 \text{ g m}^{-3}$) per temperature class ($^{\circ}\text{C}$) for the epipelagic (a) and mesopelagic (b) layers

1990), capelin (Gjørseter and Båmstedt 1998) or herring (Dragesund et al. 1997)] that migrate between different habitats for spawning, feeding and wintering. Pre-spawning polar cod were already present in the Amundsen Gulf in October and November, about 3–4 months before the aggregation started to form in Franklin Bay (Benoit et al. 2008), i.e. 2–3 months prior to the presumed start of the spawning migration. Assuming an active long-distance migration of a distant polar cod population, little polar cod biomass would have been found in the Amundsen Gulf during our survey. However, for most of the year, adult polar cod were distributed rather continuously along the Mackenzie shelf-break and in the Amundsen Gulf, occupying the same or similar water masses as during the under-ice aggregation period.

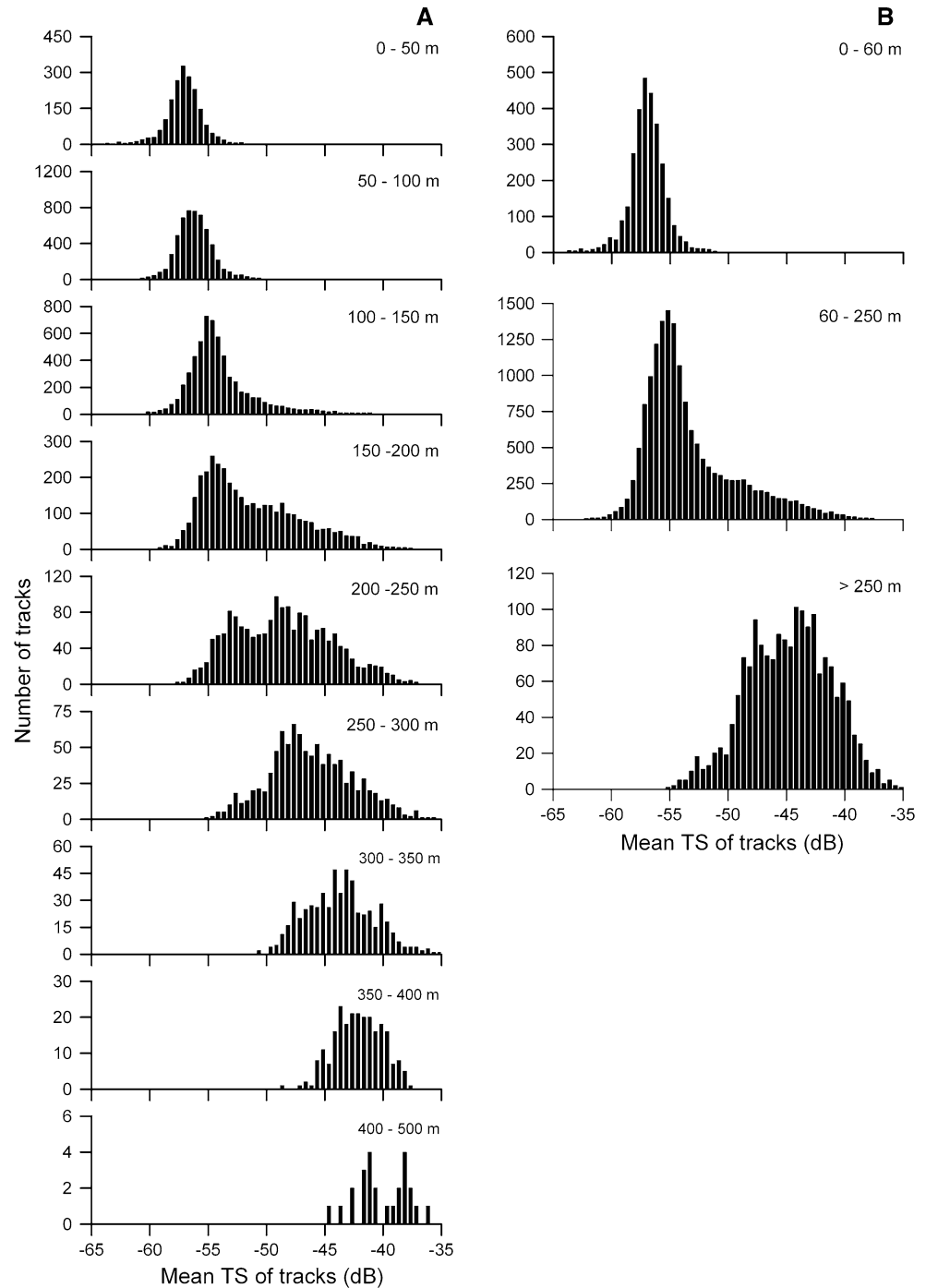
Moreover, given the low temperatures the polar cod experienced, one could expect their swimming activity to be reduced compared with other migrating species (He 1991; Campbell et al. 2008). Considering all this, we believe that an active long-distance migration is very unlikely in the case of polar cod. It is more likely that polar cod could undertake short-distance displacements just prior to concentrating on the slope and spawn. As observed for Atlantic cod (Rose et al. 1995), polar cod displacement could vary daily, alternating between days of high and low movements. Geoffroy et al. (2011) showed that under the winter ice cover in the Amundsen Gulf, polar cod form several aggregations on the slope, suggesting a patchy

distribution, which could result from such variable active displacements and residual currents. Further research on this migration and aggregation question should include electronic tagging (e.g. Comeau et al. 2002; Windle and Rose 2005) to provide estimations of the distance polar cod can migrate in an effort to test several migration hypotheses.

Implications for ecosystem functioning

What drives polar cod to distribute along slopes? Abrupt topographies often present favourable conditions for feeding of fish by concentrating zooplankton prey under the influence of ocean currents (e.g. Mackas et al. 1997; Genin 2004; Cotté and Simard 2005; Cartes et al. 2009). Since polar cod were limited in feeding abilities during winter (Benoit et al. 2010), one could expect them to feed more intensively during the open-water season, to acquire the energy needed for the development of gonads. Sparser distribution might also reduce inter-individual competition and possibly improve feeding capacities in food-limited environments (Eggers 1976; Hop et al. 1997). The main preys of polar cod in the southeastern Beaufort Sea in the following winter were the older stages of large copepods (*Calanus glacialis*, *Calanus hyperboreus*, and *Metridia longa*) (Benoit et al. 2010). From September to November, these three species dominate ($>75\%$) the zooplankton biomass in the southeastern Beaufort Sea (Forest et al. 2007; Darnis et al. 2008; Geoffroy et al. 2011) and have their highest biomasses below the Cold Halocline ($>150 \text{ m}$) (Ashjian et al. 2005; Geoffroy et al. 2011). Hence, by concentrating at the slope, polar cod likely increase the possibility of finding higher concentrations of their copepod prey species. During our study period, the oldest stages of *C. glacialis*, *C. hyperboreus* and *M. longa* were present at all water depths, with highest carbon content between 400 and 700 m (Suzuki K, Department of Biology, Université Laval, personal communication). This peak zooplankton density overlaps the deep distribution of high polar cod biomass. Cartes et al. (2009) suggested that offshore mesopelagic prey could sustain the fish aggregations often observed at shelf-breaks. Upward displacement of isohalines and isotherms observed at shelf-breaks reflects upwelling conditions on the Mackenzie shelf and in the Amundsen Gulf. Resulting onshore currents impinging on the bottom possibly steered zooplankton onto slope areas, a phenomenon that has already been observed in other marine systems (e.g. Simard et al. 1986; Mackas et al. 1997; Cotté and Simard 2005). In September–October 2002, copepod prey species of polar cod were also more abundant in the central Amundsen Gulf than on the Mackenzie shelf (Darnis et al. 2008). The recurrence of high primary production in the central Amundsen Gulf during

Fig. 9 In situ target strength (TS, in dB) frequency distribution by 50-m depth intervals (a) and for the epipelagic layer (depths < 60 m), and upper (60–250 m depths) and deeper (>250 m depths) mesopelagic layers (b). TS values are means of split-beam single-target tracks



fall (Brugel et al. 2009; Ardyna et al. 2011) may locally cascade through the trophic web. The Amundsen Gulf could then provide good feeding conditions for pre-spawning polar cod. Further investigation including local zooplankton and current data is needed to verify the concentration mechanism we suggest. Distribution of polar cod along slopes would also force its predators to concentrate their feeding efforts in the same areas. The fact that belugas, which are predators of polar cod, mostly distribute

along slopes in spring in the southeastern Beaufort Sea (Asselin et al. 2011), lends support to this assumption.

Summary

- This study describes the large-scale distribution of polar cod biomass in the southeastern Beaufort Sea,

- Through the in situ TS analysis, we evidenced the depth segregation of polar cod sizes and their association with warmer waters,
- Our biomass estimates showed that adult polar cod densities in Amundsen Gulf compare with that of rich areas such as the Barents Sea,
- We bring support to the assumption by Geoffroy et al. (2011) that dense aggregations do not form until the ice cover is consolidated,
- We showed that polar cod distributes continuously along slopes and that the Amundsen Gulf would be the source for aggregations that form in winter.
- Further research is needed to understand the precise mechanisms for the formation of these aggregations and the role they play in the life cycle of polar cod. Special attention should be given to fish sampling in order to assess biological parameters of polar cod (e.g. feeding intensities and state of gonads), crucial information for a comprehensive knowledge of the ecology of this key forage species.

Acknowledgments This study was conducted within the framework of the Canadian Arctic Shelf Exchange Study (CASES), a Research Network funded by the Natural Sciences and Engineering Research Council of Canada (NSERC) and the Canada Foundation for Innovation. We thank the officers and crew of the CCGS *Amundsen* for enthusiastic and professional assistance at sea, and the team of technicians, assistants and colleagues who contributed to the collection of acoustic data. Special thanks to Y. Gratton for the validated physical data and Caroline Bouchard for photographs of polar cod juveniles. This is a contribution to the program of Québec-Océan, the Canada Research Chair on the Response of Marine Arctic Ecosystems to Climate Warming at Université Laval, and the Fisheries and Oceans Canada Research Chair in Underwater Acoustics Applied to Ecosystem and Marine Mammals at ISMER-UQAR.

References

- Aagaard K (1984) The Beaufort undercurrent. In: Barnes PW, Schell DM, Reimnitz E (eds) *The Alaskan Beaufort Sea: ecosystems and environments*. Academic Press, Orlando, pp 47–71
- Ardyna M, Gosselin M, Michel C, Poulin M, Tremblay JE (2011) Environmental forcing of phytoplankton community structure and function in the Canadian High Arctic: contrasting oligotrophic and eutrophic regions. *Mar Ecol Prog Ser* 442:37–57. doi:10.3354/meps09378
- Ashjian CJ, Gallager SM, Plourde S (2005) Transport of plankton and particles between the Chukchi and Beaufort Seas during summer 2002, described using a Video Plankton Recorder. *Deep Sea Res Part II Top Stud Oceanogr* 52:3259–3280. doi:10.1016/j.dsr2.2005.10.002
- Asselin N, Barber D, Stirling I, Ferguson S, Richard P (2011) Beluga (*Delphinapterus leucas*) habitat selection in the eastern Beaufort Sea in spring, 1975–1979. *Polar Biol* 34:1973–1988. doi:10.1007/s00300-011-0990-5
- Barber DG, Hanesiak JM (2004) Meteorological forcing of sea ice concentrations in the southern Beaufort Sea over the period 1979 to 2000. *J Geophys Res Oceans* 109:C06014. doi:10.1029/2003jc002027
- Barber DG, Asplin MG, Gratton Y, Lukovich JV, Galley RJ, Raddatz RL, Leitch D (2010) The International Polar Year (IPY) Circumpolar Flaw Lead (CFL) system study: overview and the physical system. *Atmos Ocean* 48:225–243. doi:10.3137/oc317.2010
- Benoit D, Simard Y, Fortier L (2008) Hydroacoustic detection of large winter aggregations of Arctic cod (*Boreogadus saida*) at depth in ice-covered Franklin Bay (Beaufort Sea). *J Geophys Res Oceans* 113:C06S90. doi:10.1029/2007JC004276
- Benoit D, Simard Y, Gagné J, Geoffroy M, Fortier L (2010) From polar night to midnight sun: photoperiod, seal predation, and the diel vertical migrations of polar cod (*Boreogadus saida*) under landfast ice in the Arctic Ocean. *Polar Biol* 33:1505–1520. doi:10.1007/s00300-010-0840-x
- Bouchard C, Fortier L (2008) Effects of polynyas on the hatching season, early growth and survival of polar cod *Boreogadus saida* in the Laptev Sea. *Mar Ecol Prog Ser* 355:247–256. doi:10.3354/meps07335
- Bradstreet MSW, Finley KJ, Sekerak AD, Griffiths WB, Evans CR, Fabijan MF, Stallard HE (1986) Aspects of the biology of arctic cod (*Boreogadus saida*) and its importance in arctic marine food chains. *Can Tech Rep Fish Aquat Sci* 1491
- Brugel S, Nozais C, Poulin M, Tremblay JE, Miller LA, Simpson KG, Gratton Y, Demers S (2009) Phytoplankton biomass and production in the southeastern Beaufort Sea in autumn 2002 and 2003. *Mar Ecol Prog Ser* 377:63–77. doi:10.3354/meps07808
- Campbell HA, Fraser KPP, Bishop CM, Peck LS, Egginton S (2008) Hibernation in an Antarctic fish: on ice for winter. *PLoS ONE* 3:e1743. doi:10.1371/journal.pone.0001743
- Carmack EC, Macdonald RW (2002) Oceanography of the Canadian Shelf of the Beaufort Sea: a setting for marine life. *Arctic* 55:29–45
- Cartes JE, Hidalgo M, Papiol V, Massuti E, Moranta J (2009) Changes in the diet and feeding of the hake *Merluccius merluccius* at the shelf-break of the Balearic Islands: influence of the mesopelagic-boundary community. *Deep Sea Res Part I Oceanogr Res Pap* 56:344–365. doi:10.1016/j.dsr.2008.09.009
- Comeau LA, Campana SE, Castonguay M (2002) Automated monitoring of a large-scale cod (*Gadus morhua*) migration in the open sea. *Can J Fish Aquat Sci* 59:1845–1850. doi:10.1139/f02-152
- Cotté C, Simard Y (2005) Formation of dense krill patches under tidal forcing at whale feeding hot spots in the St. Lawrence Estuary. *Mar Ecol Prog Ser* 288:199–210. doi:10.3354/meps288199
- Craig PC, Griffiths WB, Haldorson L, McElderry H (1982) Ecological studies of Arctic cod (*Boreogadus saida*) in Beaufort Sea coastal waters, Alaska. *Can J Fish Aquat Sci* 39:395–406. doi:10.1139/f82-057
- Crawford RE, Jorgenson JK (1996) Quantitative studies of Arctic cod (*Boreogadus saida*) schools: important energy stores in the Arctic food web. *Arctic* 49:181–193
- Cross WE (1982) Under ice biota at the Pond Inlet edge and in adjacent fast ice areas during spring. *Arctic* 35:13–27
- Darnis G, Barber DG, Fortier L (2008) Sea ice and the onshore-offshore gradient in pre-winter zooplankton assemblages in southeastern Beaufort Sea. *J Mar Syst* 74:994–1011. doi:10.1016/j.jmarsys.2007.09.003
- Dragesund O, Johannessen A, Ulltang Ø (1997) Variation in migration and abundance of Norwegian spring spawning herring (*Clupea harengus* L.). *Sarsia* 82:97–105. doi:10.1080/00364827.1997.10413643
- Eggers DM (1976) Theoretical effect of schooling by planktivorous fish predators on rate of prey consumption. *J Fish Res Board Can* 33:1964–1971. doi:10.1139/f76-250

- Falk-Petersen IB, Frivoll V, Gulliksen B, Haug T (1986) Occurrence and size age relations of polar cod, *Boreogadus saida* (Lepechin), in Spitsbergen coastal waters. *Sarsia* 71:235–245. doi:10.1080/00364827.1986.10419693
- Foote KG, Knudsen HP, Vestnes G, MacLennan DN, Simmonds EJ (1987) Calibration of acoustic instruments for fish density estimation: a practical guide. ICES Coop Res Rep 144
- Forest A, Sampei M, Hattori H, Makabe R, Sasaki H, Fukuchi M, Wassmann P, Fortier L (2007) Particulate organic carbon fluxes on the slope of the Mackenzie Shelf (Beaufort Sea): physical and biological forcing of shelf-basin exchanges. *J Mar Syst* 68:39–54. doi:10.1016/j.jmarsys.2006.10.008
- Francois RE, Garrison GR (1982) Sound-absorption based on ocean measurements. 2—Boric-acid contribution and equation for total absorption. *J Acoust Soc Am* 72:1879–1890. doi:10.1121/1.388673
- Galley RJ, Key E, Barber DG, Hwang BJ, Ehn JK (2008) Spatial and temporal variability of sea ice in the southern Beaufort Sea and Amundsen Gulf: 1980–2004. *J Geophys Res Oceans* 113. doi:10.1029/2007JC004553
- Genin A (2004) Bio-physical coupling in the formation of zooplankton and fish aggregations over abrupt topographies. *J Mar Syst* 50:3–20. doi:10.1016/j.marsys.2003.10.008
- Geoffroy M, Robert D, Darnis G, Fortier L (2011) The aggregation of polar cod (*Boreogadus saida*) in the deep Atlantic layer of ice-covered Amundsen Gulf (Beaufort Sea) in winter. *Polar Biol* 34:1959–1971. doi:10.1007/s00300-011-1019-9
- Gjørøseter H, Båmstedt U (1998) The population biology and exploitation of capelin (*Mallotus villosus*) in the Barents Sea. *Sarsia* 83:453–496. doi:10.1080/00364827.1998.10420445
- Gjørøseter H, Bogstad B, Tjelmeland S (2009) Ecosystem effects of the three capelin stock collapses in the Barents Sea. *Mar Biol Res* 5:40–53. doi:10.1080/1745100802454866
- He PG (1991) Swimming endurance of the Atlantic cod, *Gadus morhua* L., at low temperatures. *Fish Res* 12:65–73. doi:10.1016/0165-7836(91)90050-P
- Holliday DV, Pieper RE (1995) Bioacoustical oceanography at high frequencies. *ICES J Mar Sci* 52:279–296. doi:10.1016/1054-3139(95)80044-1
- Hop H, Graham M, Trudeau VL (1995) Spawning energetics of Arctic cod (*Boreogadus saida*) in relation to seasonal development of the ovary and plasma sex steroid-levels. *Can J Fish Aquat Sci* 52:541–550. doi:10.1139/f95-055
- Hop H, Welch HE, Crawford RE (1997) Population structure and feeding ecology of Arctic cod (*Boreogadus saida*) schools in the Canadian High Arctic. In: Reynolds J (ed) *Fish Ecology in Arctic North America*, Fairbanks, Alaska, 19–21 May 1992. *Am Fish Soc Symp* 19, Bethesda, Maryland, pp 68–80
- Horne JK (2000) Acoustic approaches to remote species identification: a review. *Fish Oceanogr* 9:356–371. doi:10.1046/j.1365-2419.2000.00143.x
- Hovgård H, Christensen S (1990) Population structure and migration patterns of Atlantic cod (*Gadus morhua*) in west Greenland waters based on tagging experiments from 1946 to 1964. *NAFO Sci Coun Stud* 45–50
- Jarvela LE, Thorsteinson LK (1999) The epipelagic fish community of Beaufort Sea coastal waters, Alaska. *Arctic* 52:80–94
- Kang M, Furusawa M, Miyashita K (2002) Effective and accurate use of difference in mean volume backscattering strength to identify fish and plankton. *ICES J Mar Sci* 59:794–804. doi:10.1006/jmsc.2002.1229
- Kulikov EA, Carmack EC, Macdonald RW (1998) Flow variability at the continental shelf break of the Mackenzie Shelf in the Beaufort Sea. *J Geophys Res Oceans* 103:12725–12741. doi:10.1029/97JC03690
- Lafrance P (2009) Saison d'éclosion et survie des stades larvaires et juvéniles chez la morue arctique (*Boreogadus saida*) du sud-est de la mer de Beaufort. Université Laval, Québec
- Lanos R (2009) Circulation régionale, masses d'eau, cycles d'évolution et transports entre la mer de Beaufort et le golfe d'Amundsen. Université du Québec—INRS, Eau, Terre et Environnement, Québec
- Lavery AC, Wiebe PH, Stanton TK, Lawson GL, Benfield MC, Copley N (2007) Determining dominant scatterers of sound in mixed zooplankton populations. *J Acoust Soc Am* 122:3304–3326. doi:10.1121/1.2793613
- Logerwell E, Wilson C (2004) Species discrimination of fish using frequency-dependent acoustic backscatter. *ICES J Mar Sci* 61:1004–1013. doi:10.1016/j.icesjms.2004.04.004
- Lønne OJ, Gulliksen B (1989) Size, age and diet of polar cod, *Boreogadus saida* (Lepechin 1773), in ice covered waters. *Polar Biol* 9:187–191
- Lowry LF, Frost KJ (1981) Distribution, growth, and foods of Arctic cod (*Boreogadus saida*) in the Bering, Chukchi, and Beaufort seas. *Can Field Nat* 95:186–191
- Lukovich JV, Barber DG (2006) Atmospheric controls on sea ice motion in the southern Beaufort Sea. *J Geophys Res Atmos* 111:D18103. doi:10.1029/2005JD006408
- Mackas DL, Kieser R, Saunders M, Yelland DR, Brown RM, Moore DF (1997) Aggregation of euphausiids and Pacific hake (*Merluccius productus*) along the outer continental shelf off Vancouver Island. *Can J Fish Aquat Sci* 54:2080–2096
- Madureira LSP, Everson I, Murphy EJ (1993) Interpretation of acoustic data at 2 frequencies to discriminate between Antarctic Krill (*Euphausia superba dana*) and other scatterers. *J Plankton Res* 15:787–802. doi:10.1093/plankt/15.7.787
- Michaud J, Fortier L, Rowe P, Ramseier R (1996) Feeding success and survivorship of Arctic cod larvae, *Boreogadus saida*, in the northeast water polynya (Greenland sea). *Fish Oceanogr* 5:120–135
- Murase H, Ichihara M, Yasuma H, Watanabe H, Yonezaki S, Nagashima H, Kawahara S, Miyashita K (2009) Acoustic characterization of biological backscatterings in the Kuroshio-Oyashio inter-frontal zone and subarctic waters of the western North Pacific in spring. *Fish Oceanogr* 18:386–401. doi:10.1111/j.1365-2419.2009.00519.x
- Ona E (1999) Methodology for target strength measurements (with special reference to in situ techniques for fish and mikro-nekton). *ICES Coop Res Rep* 235
- Parker-Stetter S, Horne J, Weingartner T (2011) Distribution of polar cod and age-0 fish in the U.S. Beaufort Sea. *Polar Biol* 34:1543–1557. doi:10.1007/s00300-011-1014-1
- Pickart RS (2004) Shelfbreak circulation in the Alaskan Beaufort Sea: mean structure and variability. *J Geophys Res Oceans* 109:C04024. doi:10.1029/2003jc001912
- Ponomarenko VP (1968) Some data on the distribution and migrations of polar cod in the seas of the Soviet Arctic. *Rapp Procès Verbaux Réunions CIEM* 158:131–135
- Ponomarenko VP (2000) Eggs, larvae, and juveniles of polar cod *Boreogadus saida* in the Barents, Kara, and White Seas. *J Ichthyol* 40:165–173
- Rand K, Logerwell E (2010) The first demersal trawl survey of benthic fish and invertebrates in the Beaufort Sea since the late 1970s. *Polar Biol* 34:475–488. doi:10.1007/s00300-010-0900-2
- Rass TS (1968) Spawning and development of polar cod. *Rapp Procès Verbaux Réunions CIEM* 158:135–137
- Rose GA, Deyoung B, Colbourne EB (1995) Cod (*Gadus morhua* L.) migration speeds and transport relative to currents on the Northeast Newfoundland shelf. *ICES J Mar Sci* 52:903–913. doi:10.1006/jmsc.1995.0087
- Sekerak AD (1982) Young-of-the-year cod (*Boreogadus*) in Lancaster Sound and Western Baffin Bay. *Arctic* 35:75–87

- Simard Y, Lavoie D (1999) The rich krill aggregation of the Saguenay—St. Lawrence Marine Park: hydroacoustic and geo-statistical biomass estimates, structure, variability, and significance for whales. *Can J Fish Aquat Sci* 56:1182–1197. doi:[10.1139/f99-063](https://doi.org/10.1139/f99-063)
- Simard Y, Sourisseau M (2009) Diel changes in acoustic and catch estimates of krill biomass. *ICES J Mar Sci* 66:1318–1325. doi:[10.1093/icesjms/fsp055](https://doi.org/10.1093/icesjms/fsp055)
- Simard Y, Deladurantaye R, Therriault JC (1986) Aggregation of euphausiids along a coastal shelf in an upwelling environment. *Mar Ecol Prog Ser* 32:203–215
- Simard Y, McQuinn I, Montminy M, Lang C, Miller D, Stevens C, Wiggins D, Marchalot C (1997) Description of the HAC format for raw and edited hydroacoustic data, version 1.0. *Can Tech Rep Fish Aquat Sci* 2174
- Simard Y, McQuinn I, Montminy M, Lang C, Stevens C, Goulet F, Lapierre J-P, Beaulieu J-P, Landry J, Samson Y, Gagné M (2000) CH2, Canadian Hydroacoustic data analysis tool 2 user's manual (Version 2.0). *Can Tech Rep Fish Aquat Sci* 2332
- Simmonds EJ, MacLennan DN (2005) Fisheries acoustics: theory and practice. *Fish and Aquatic Resources Series*, 2 edn. Blackwell Science, Oxford
- Welch HE, Bergmann M, Siferd TD, Martin KA, Curtis MF, Crawford RE, Conover RJ, Hop H (1992) Energy flow through the marine ecosystem of the Lancaster Sound Region, Arctic Canada. *Arctic* 45:343–357
- Welch HE, Crawford RE, Hop H (1993) Occurrence of Arctic cod (*Boreogadus saida*) schools and their vulnerability to predation in the Canadian High Arctic. *Arctic* 46:331–339
- Windle MJS, Rose GA (2005) Migration route familiarity and homing of transplanted Atlantic cod (*Gadus morhua*). *Fish Res* 75:193–199. doi:[10.1016/j.fishres.2005.05.006](https://doi.org/10.1016/j.fishres.2005.05.006)